

Temperature dependent coercivity crossover in pseudo-spin-valve magnetic tunnel junctions with perpendicular anisotropy

G. Feng,^{1,2,a)} H. C. Wu,^{1,b)} J. F. Feng,¹ and J. M. D. Coey¹¹CRANN and School of Physics, Trinity College, Dublin 2, Ireland²Magnetic Materials Group, National Institute of Standards and Technology (NIST), Gaithersburg, Maryland 20899, USA

(Received 15 March 2011; accepted 18 June 2011; published online 26 July 2011)

We report the temperature dependent collapse of tunnel magnetoresistance (TMR) in perpendicular anisotropy magnetic tunnel junctions (pMTJs) with AlO_x barriers and $(\text{Co/Pt})_3$ multilayer electrodes, due to the coercivity crossover of the top and bottom $(\text{Co/Pt})_3$ stacks. The different temperature dependence of two $(\text{Co/Pt})_3$ stacks in pMTJs is mainly caused by the additional perpendicular anisotropy created at interface between the ferromagnetic electrode and the AlO_x barrier. © 2011 American Institute of Physics. [doi:10.1063/1.3614000]

Magnetic tunnel junctions with perpendicular anisotropy (pMTJs) are of interest because of their potential applications in spin-transfer torque magnetoresistive random access memory (STT-MRAM).^{1–3} Compared to STT devices with in-plane anisotropy, perpendicular anisotropy spin valves and magnetic tunnel junctions offer reduced critical switching current density as well as high thermal stability at small cell size.⁴ Furthermore, circular shapes can be used in perpendicular magnetic elements because the thermal stability is controlled by intrinsic magnetostatic and interface anisotropy without depending on shape anisotropy. Magnetic multilayering is one way to achieve perpendicular magnetic anisotropy. Co/Pd, Co/Pt, Co/Au, and Co/Ni multilayers all show perpendicular anisotropy for certain ranges of thickness and period.^{5–9} Lots of studies have been carried out on the fabrication and characterization of pMTJs with AlO_x and MgO barriers.^{10–14} Promising progress has been made not only on reaching high tunneling magnetoresistance (TMR) ratios but also achieving a low critical current density.^{15–17} Here, we report a temperature dependent effect: coercivity crossover. The TMR of pMTJs with a pseudo spin valve structure disappears in a narrow temperature range, only to reappear at lower temperature.

The pMTJ stacks Ta 10/Pt 10/((Co 0.7/Pt 2.0)₂/Co 0.7/ AlO_x 2.0/((Co 0.4/Pt 2.0)₃/Ta 5 (unit in nm) were grown on thermally oxidized Si substrates by magnetron sputtering in a Shamrock deposition system. The AlO_x barrier layer was deposited by radiofrequency sputtering directly from Al_2O_3 targets in the target-facing-target configuration. Junctions with sizes of $8 \times 8 \mu\text{m}^2$ were fabricated using UV-lithography and Ar ion-milling techniques. The magneto-transport and magnetic properties were characterized by a standard four-point method in a Quantum Design Physical Property Measurement System at temperatures ranging from 10 K to 300 K. The magnetic field is applied perpendicular to the plane of pMTJ stacks during all measurements.

In Co/Pt multilayers, the coercivity can be easily tuned by modifying the thickness of Co layers or changing the repetition number of the $(\text{Co/Pt})_n$ stack. Here, we fix the repeti-

tion (n) as 3 and use different Co thicknesses in order to vary coercivity (H_c) and separate the soft and hard layer switches. In our pMTJ stacks, the top $(\text{Co 0.4/Pt 2.0})_3$ serves as the soft layer since it has a smaller H_c at room temperature compared to that of the bottom $(\text{Co 0.7/Pt 2.0})_3$ layer according to our previous study.⁸

Under a bias voltage of 20 mV, a typical pMTJ device shows a tunnel magnetoresistance of up to 9% and 25% at room temperature and 50 K, respectively, as shown in Fig. 1. The switching fields at room temperature are 50.8 and 96.4 mT, corresponding to H_c of the soft and hard ferromagnetic layers. Both coercivities increase with decreasing temperature.

The insert of Fig. 1 shows the bias dependence of TMR ratio at room temperature and 50 K. The TMR decreases with increasing bias voltage and a $V_{1/2}$ of 400 mV, at which the TMR value is decreased to half of its maximum value, is measured at room temperature. This value decreases to 330 mV at 50 K. $V_{1/2}$ in the pMTJ devices is smaller than that of in-plane anisotropy MTJs with AlO_x barriers, where it usually exceeds 600 mV at room temperature.¹⁸ This may indicate that AlO_x barrier quality is poorer in the pMTJ stacks. In order to achieve strong perpendicular magnetic anisotropy, we used 10 nm Pt as a seed layer to induce good (111) texture for Co/Pt multilayers, but this may increase the roughness of the whole stack, especially at the bottom interface between the Co/Pt electrode and the AlO_x barrier.

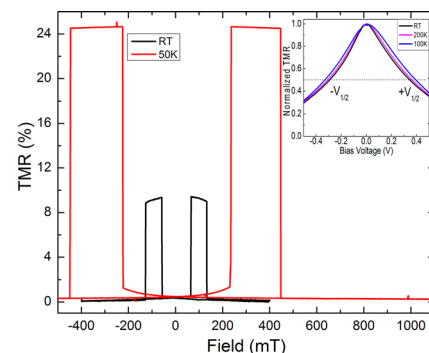


FIG. 1. (Color online) Out of plane TMR curves at room temperature and 50 K. The inset shows the bias dependence of the TMR ratio at these temperatures.

^{a)}Electronic mail: gen.feng@nist.gov.

^{b)}Electronic mail: wuhc@tcd.ie.

Figure 2 shows the TMR ratio and the junction resistance for the pMTJ as a function of temperature. The resistance for both parallel and anti-parallel configurations increases when temperature decreases. This is characteristic of tunneling behavior. The resistance-area (RA) product of the pMTJ junction shown in Fig. 2 is $5.5 \times 10^5 \Omega \mu\text{m}^2$ (for the parallel configuration at room temperature), which is reasonable for a 2.0 nm AlO_x barrier. The RA product increases to $6.3 \times 10^5 \Omega \mu\text{m}^2$ at 10 K. However, the change of resistance for the anti-parallel configuration is different from that for the parallel configuration. A sudden decrease of resistance is observed between 210 K and 200 K. The RA product for the anti-parallel configuration is around $6.0 \times 10^5 \Omega \mu\text{m}^2$ at room temperature and increases to $6.7 \times 10^5 \Omega \mu\text{m}^2$ at 215 K but then decreases to $5.9 \times 10^5 \Omega \mu\text{m}^2$ at 210 K. In the same temperature region, from 210 K to 200 K, the RA products for the anti-parallel configuration and parallel configuration are very similar, so the TMR disappears. The RA product for the anti-parallel configuration starts to recover below 195 K, reaching $6.9 \times 10^5 \Omega \mu\text{m}^2$, and it then becomes higher than for the parallel configuration ($6.0 \times 10^5 \Omega \mu\text{m}^2$). Further decreasing temperature from 195 K to 10 K results in a continuous resistance change for the anti-parallel configuration, which is similar to that for parallel configuration. The temperature dependence of TMR ratio follows the same tendency, it increases from 9% at 300 K to 14% at 215 K, and suddenly decreases to almost zero at 210 K, and then comes back to normal below 195 K, reaching 26% at 10 K.

A detailed field scan in the temperature region from 180 K to 225 K was then carried out, as shown in Fig. 3(a). The pMTJ shows well defined switching fields of 132 mT and 161 mT for the soft and hard Co/Pt multilayers at 225 K. When the temperature decreases to 215 K, however, the switch under the negative fields disappears, although the TMR remains in the positive field branch. At 210 K, the switches for both negative and positive field branches disappear, resulting in the sudden collapse of TMR. The TMR recovers, back to 15%, when the temperature is decreased further to 195 K. However, the TMR peak is very sharp on the positive field branch due to the small coercivity difference between the soft and hard magnetic layers. At 180 K, a typical pseudo-spin-valve type TMR curve comes back. Fig. 3(b) summarizes the coercivity for both top and bottom Co/Pt electrodes from room temperature to 10 K, and a clear coercivity crossover is seen in the relevant temperature range. The TMR collapse in the coercivity crossover region may suggest that the top and bottom Co/Pt layers couple to

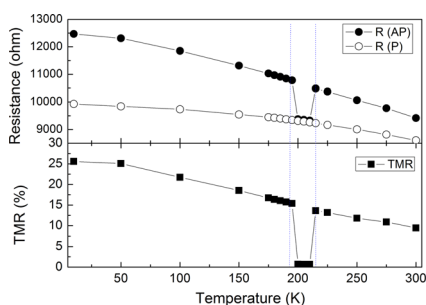


FIG. 2. (Color online) Temperature dependence of the TMR ratio and junction resistance.

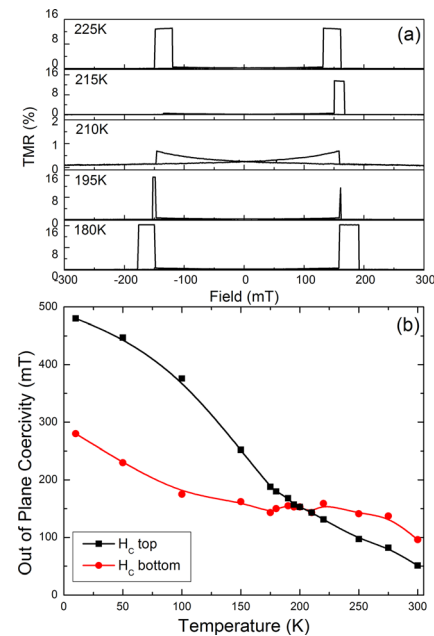


FIG. 3. (Color online) (a) Out of plane TMR curves at temperatures ranging from 180 K to 225 K (b) Temperature dependence of coercivity for top and bottom $(\text{Co/Pt})_3$ multilayers.

each other and switch simultaneously resulting in the lack of any well defined anti-parallel configuration.

The magnetic properties of unpatterned pMTJ stacks have also been characterized at different temperatures. The coercivity for the top and bottom electrodes of unpatterned pMTJ stack is plotted in Fig. 4(a) as the function of temperature. A coercivity crossover similar to that of patterned pMTJs is observed. The inset of Fig. 4(a) presents the corresponding M-H curves at different temperatures. The crossover temperature region occurs around 150 K, which is lower than that of the patterned pMTJ samples. This is probably related to the dipole field generated by micrometer-sized MTJ pillars after patterning. It is noted that a magnetic switch can be observed at low field for all the M-H curves measured at temperatures below 200 K. The origin of this switch is unclear and it might indicate the presence of cobalt oxides in our pMTJ stacks.

In order to further understand the origin of the coercivity crossover in our pMTJ samples, we also measured the magnetic properties of the $(\text{Co}_x/\text{Pt } 2.0)_3$ multilayers without the AlO_x barrier on either side, as shown in Fig. 4(b). The multilayers were deposited on the thermal-oxidized silicon substrate with additional 2.0 nm Pt as the seed layer. The thickness x of the Co layer was varied from 0.4 nm to 0.7 nm with a step of 0.1 nm. At room temperature, $(\text{Co } 0.7/\text{Pt } 2.0)_3$ shows the highest coercivity and $(\text{Co } 0.4/\text{Pt } 2.0)_3$ has the lowest. The coercivities for all four studied samples increase with decreasing temperature and reach almost same value (96 mT) at 10 K. No crossover is observed between 300 K and 10 K. It is also noticed that the coercivity of both $(\text{Co } 0.4/\text{Pt } 2.0)_3$ and $(\text{Co } 0.7/\text{Pt } 2.0)_3$ increases when an AlO_x layer is deposited on top. The results indicate that the AlO_x barrier plays an important role in determining the coercivity.

The deposition of the AlO_x barrier either on top or beneath the Co/Pt multilayers affects the magnetic anisotropy. As an approximation, K_{\perp}^{eff} in our pMTJs stack can be written as¹⁹

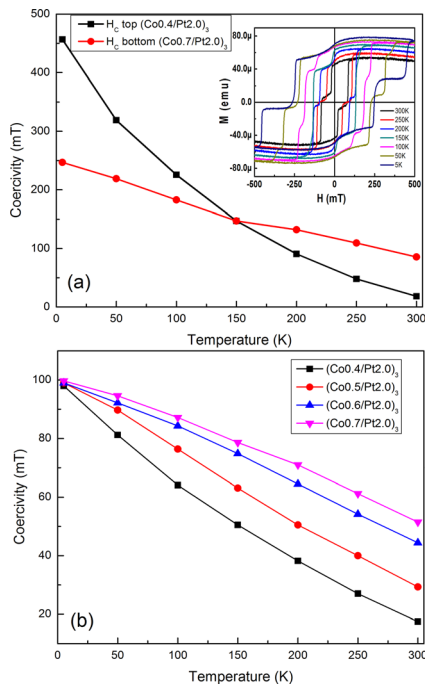


FIG. 4. (Color online) (a) Temperature dependence of coercivity for unpatterned pMTJ stack and (b) for $(\text{Co } x/\text{Pt } 2.0)_3$ multilayer with $x=0.4, 0.5, 0.6, 0.7$ (nm). The inset in (a) shows the corresponding magnetization versus magnetic field (M - H) curves at different temperatures.

$$K_{\perp}^{\text{eff}} = K_V^{\text{Co}} + \frac{(2n-1)K_S^{\text{Co/Pt}}}{nt_{\text{Co}}} + \frac{K_S^{\text{Co/AlO}_x}}{nt_{\text{Co}}},$$

where K_V^{Co} is the volume anisotropy of the cobalt, which includes the shape and magnetocrystalline anisotropy, and $K_S^{\text{Co/Pt}}$ is the interfacial anisotropy of the Co/Pt bilayer. $K_S^{\text{Co/AlO}_x}$ is the interfacial anisotropy between ferromagnetic layer and tunnel barrier. Interfacial perpendicular anisotropy between oxide and ferromagnetic metal has been observed in a Pt/Co/AlO_x multilayer.²⁰ The magnitude of $K_S^{\text{Co/AlO}_x}$ is related to the density of Co-O bonding at the Co/AlO_x interface and can be attributed to hybridization between Co 3d and O 2p orbitals. By extrapolating the magnetization curves of $(\text{Co } x/\text{Pt } 2.0)_3$ multilayers ($x=0.3$ to 0.8 nm), the anisotropy field H_K and $K_{\perp}^{\text{eff}} = \frac{1}{2}\mu_0 M_S H_K$ were obtained. The product of $K_{\perp}^{\text{eff}} \times t_{\text{Co}}$ decreases linearly with t_{Co} and the linear fit to the data yields $K_S^{\text{Co/Pt}} = 0.31$ mJ/m² and $K_V^{\text{Co}} = 3.10 \times 10^4$ J/m³. The effective magnetic anisotropy for the stack of AlO_x/(Co x /Pt 2.0)₃, which is identical to that top layer in the studied pMTJs, is 5.18×10^5 J/m³. Then by using Eq. (1), the interfacial magnetic anisotropy of the AlO_x/Co interface is determined. The result, $K_S^{\text{Co/AlO}_x} = 0.37$ mJ/m², indicates that interfacial anisotropy ($K_S^{\text{Co/AlO}_x}$) between ferromagnetic metal and barrier is larger than that of ferromagnetic metal and non-magnetic interface anisotropy ($K_S^{\text{Co/Pt}}$). Our observation is consistent with the recent report that the interfacial anisotropy between MgO and CoFeB is strong enough to maintain a 1.3 to 1.7 nm CoFeB layer perpendicular.^{17,21} The observed coercivity crossover is mainly from the interfacial anisotropy between ferromagnetic Co and the AlO_x tunnel barrier. The top interfacial anisotropy has stronger temperature dependence according to the results shown in Figs. 3 and 4(a).

In summary, we have observed the temperature dependent collapse of TMR in a pseudo-spin-valve type pMTJ, due to the coercivity crossover of the top and bottom $(\text{Co/Pt})_3$ electrodes. The pMTJ devices show a TMR ratio of up to 9% at room temperature, with the switching fields of 51 and 96 mT for the top and bottom $(\text{Co/Pt})_3$ layers. The TMR increases to 14% at 215 K, but in the temperature range from 200 K to 210 K, it disappears because the coercivity of two ferromagnetic layers crosses. The TMR recovers below 190 K and reaches 26% at 10 K. Temperature dependent coercivity crossover is mainly caused by the additional interfacial perpendicular anisotropy created at the ferromagnetic electrode and the AlO_x barrier interface.

This work was supported by SFI as part of the MANSE project 2005/IN/1850 and was conducted under the framework of the INSPIRE programme funded by the Irish Government's Programme for Research in Third Level Institutions, Cycle 4, National Development Plan 2007-2013.

- ¹N. Nishimura, T. Hirai, A. Koganei, T. Ikeda, K. Okano, Y. Sekiguchi, and Y. Osada, *J. Appl. Phys.* **91**, 5246 (2002).
- ²X. Zhu and J.-G. Zhu, *IEEE Trans. Magn.* **42**, 2739 (2006).
- ³T. Kishi, H. Yoda, T. Kai, T. Nagase, E. Kitagawa, M. Yoshikawa, K. Nishiyama, T. Daibou, M. Nagamine, M. Amano, S. Takahashi, M. Nakayama, N. Shimomura, H. Aikawa, S. Ikegawa, S. Yuasa, K. Yakushiji, H. Kubota, A. Fukushima, M. Oogane, T. Miyazaki, and K. Ando, *IEDM Tech. Dig.* 309 (2008).
- ⁴S. Mangin, D. Ravelosona, J. A. Katine, M. J. Carey, B. D. Terris, E. E. Fullerton, *Nature Mater.* **5**, 210 (2006).
- ⁵P. F. Garcia, A. D. Mcinhardt, and A. Sunna, *Appl. Phys. Lett.* **47**, 178 (1985).
- ⁶B. N. Engel, C. D. England, R. A. Vanleeuwen, M. H. Wiedmann, and C. M. Falco, *J. Appl. Phys.* **70**, 5873 (1991).
- ⁷T. Sugimoto, T. Katayama, Y. Suzuki, M. Hashimoto, Y. Nishihara, A. Itoh, and K. Kawanishi, *J. Magn. Magn. Mater.* **104-107**, 1845 (1992).
- ⁸S. van Dijken, J. Moritz, and J. M. D. Coey, *J. Appl. Phys.* **97**, 063907 (2005).
- ⁹R. Law, R. Sbiaa, T. Liew, and T. C. Chong, *Appl. Phys. Lett.* **91**, 242504 (2007).
- ¹⁰H. X. Wei, Q. H. Qin, Z. C. Wen, X. F. Han, and X. G. Zhang, *Appl. Phys. Lett.* **94**, 172902 (2009).
- ¹¹M. Yoshikawa, E. Kitagawa, T. Nagase, T. Daibou, M. Nagamine, K. Nishiyama, T. Kishi, and H. Yoda, *IEEE Trans. Magn.* **44**, 2573 (2008).
- ¹²B. Carvello, C. Ducruet, B. Rodmacq, S. Auffret, E. Gautier, G. Gaudin, and B. Dieny, *Appl. Phys. Lett.* **92**, 102508 (2008).
- ¹³J. H. Park, S. Ikeda, H. Yamamoto, H. D. Gan, K. Mizunuma, K. Miura, H. Hasegawa, J. Hayakawa, K. Ito, F. Matsukura, and H. Ohno, *IEEE Trans. Magn.* **45**, 3476 (2009).
- ¹⁴J.-H. Park, M. T. Moneck, C. Park, and J.-G. Zhu, *J. Appl. Phys.* **105**, 07D129 (2009).
- ¹⁵H. Ohmori, T. Hatori, and S. Nakagawa, *J. Appl. Phys.* **103**, 07A911 (2008).
- ¹⁶K. Mizunuma, S. Ikeda, J. H. Park, H. Yamamoto, K. Mizunuma, H. Gan, K. Miura, H. Hasegawa, J. Hayakawa, F. Matsukura, and H. Ohno, *Appl. Phys. Lett.* **95**, 232516 (2009).
- ¹⁷S. Ikeda, K. Miura, H. Yamamoto, K. Mizunuma, H. Gan, M. Endo, S. Kanai, J. Hayakawa, F. Matsukura, and H. Ohno, *Nature Mater.* **9**, 721 (2010).
- ¹⁸Y. Saito, M. Amano, K. Nakajima, S. Takahashi, M. Sagoi, and K. Inomata, *IEEE Trans. Magn.* **37**, 1979 (2001).
- ¹⁹F. Garcia, F. Fetta, S. Auffret, B. Rodmacq, and B. Dieny, *J. Appl. Phys.* **93**, 8397 (2003).
- ²⁰A. Manchon, A. Manchon, C. Ducruet, L. Lombard, S. Auffret, B. Rodmacq, B. Dieny, S. Pizzini, J. Vogel, V. Uhlir, M. Hochstrasser, and G. Panaccione, *J. Appl. Phys.* **104**, 043914 (2008).
- ²¹D. C. Worledge, G. Hu, D. W. Abraham, J. Z. Sun, P. L. Trouilloud, J. Nowak, S. Brown, M. C. Gaidis, E. J. O'Sullivan, and R. P. Robertazzi, *Appl. Phys. Lett.* **98**, 022501 (2011).